Reconfigurable Modular Soft Actuator Using Origami Structures With Self-Healing Materials

Several Technological Opportunities for Robotic Applications

By Lisbeth Mena, Seppe Terryn, Bram Vanderborght, and Concepción A. Monje

Modular designs in soft robots enable repair and reconfiguration, making soft modular robots suitable for applications where resilience, flexibility, and adaptability are critical. This paper introduces a modular soft robot (MSR) based on origami actuator modules that are manufactured from reversible polymers, e.g., self-healing polymers. This work highlights three key innovations enabled by reversible polymers for MSRs. First, their reversible bonding capacity can be utilized to create high-strength interfaces between modules relying on strong covalent bonds. These interfaces can bond and debond on demand through temperature control. This reversible joining principle is downscalable and enables reconfiguration. Second, their reversible crosslinks allow for origami-based manufacturing in the solid state, involving sequential folding and binding. This process transforms 2D structures into covalently bonded and airtight 3D structures. Finally, these reversible bonds introduce a self-healing capacity to the MSRs, enabling recovery from macroscopic damages. All of these innovations are demonstrated experimentally on modular vacuum origami-based actuator modules, showing successful self-healing and reconfiguration capabilities.

Digital Object Identifier 10.1109/MRA.2025.3533386

INTRODUCTION

MSRs have potential in the field of robotics by offering unprecedented flexibility, adaptability, and cost-effectiveness. These robots consist of multiple modules that can be assembled and disassembled by means of connectors, which makes them very versatile and highly customizable to address different tasks [1]. Unlike singular robots specifically designed for particular applications, modularity in MSRs allows them to change their shape and functionality on demand and to operate effectively in various environments and under different conditions. This makes them suitable for a wide range of applications, such as medical devices [2], [3], industrial modular soft grippers [4], [5], [6], and search and rescue operations [7], [8], [9], among others.

The performance of the MSRs is determined by the connection mechanisms in addition to the particular design of their individual modules. Various approaches have been developed to ensure reliable connections while maintaining softness in

their modular units. Among them, mechanical connections, such as pin and hole, hooks, lock and key, and shape matching, provide reliable links in modular robots [10], [11], [12], [13]. Magnetic approaches are also employed to enable swift reversible connections in MSRs [14], [15], [16]. Vacuum connections are used to create airtight seals between the modules, enhancing their adaptability [17], [18], and adhesive connections allow modules to be bonded together through glue, hot-melt, and electrostatic adhesion, among other techniques, offering high connection strength and tightness without the need for complex connection structures [19], [20].

In [21] an MSR using self-healing hydrogel material as an adhesive connector was proposed. Connection and disconnection are performed using water to activate the adhesive material. Nevertheless, the modules are not soft structures, and they need to be coated with hydrogel. A self-healing polymer based on the Diels–Alder (DA) reaction, whose capacity for multiple damage–healing cycles is demonstrated in [22], is also used for the attachment and removal of elements to reconfigure voxel-based robots [23] or tactile arrays as sensors [24]. However, in both applications, the separation of the different parts or modules is accomplished by manually cutting them.

This work presents an MSR approach in which both the connector and the modules are flexible, thanks to the use of reversible polymers in their manufacture. The proposal highlights three main innovations introduced by reversible polymers for MSR. First, reusable materials with self-healing properties will be used for both components, exploiting strong covalent bonds that are reversible to make the robot more sustainable and reconfigurable. This principle of reversibility allows for the adjustment of the balance between reagents, simplifying the reconfiguration of covalent bonds. Therefore, reversible polymer networks that can bind and rebind at an interface will be used as connectors, enabling automatic connection and disconnection of the soft modular units by controlling temperature variations, offering a more controllable and robust modularity. Second, the reversible crosslinks enable origami-based fabrication in the solid state, involving sequential folding and binding. This method transforms 2D shapes into covalently bonded and airtight 3D structures. Finally, these reversible bonds introduce a self-healing capability into the materials; therefore, the MSRs can recover from macroscopic damages.

The robot modules will be based on origami, a paper-folding technique that is currently being widely used in innovative solutions in applications such as manipulation and grasping tasks [25], [26] and biomedical [27], space [28], [29], [30], medical [31], [32], energy and communications [33], [34], and robotics [35], [36] applications. Origami robots are soft, inexpensive, and simple to prepare compared to traditional ones. Their streamlined design eliminates the need for complex gear systems, making them lightweight. They are highly foldable and space efficient, making transportation and storage easier. Additionally, the origami technique offers flexible and scalable structures. Origami robots are constructed using a flat composite material sheet that is folded at conformal joints to create a complex 3D structure. These origami patterns are natural single units, and combining them, by adding or removing some of these units, allows adaptability to different tasks or environments. Consequently, origami structures provide modular configurations.

The process of transforming an origami-based structure into a useful application begins with selecting a pattern. Table 1 presents a list of recognized origami patterns with their relevant properties.

The patterns shown in Table 1 and Figure 1 are the most commonly used in technological solutions. The Miura-ori and Flasher patterns have a folding geometry that allows them to expand along a surface and are commonly used in

TABLE 1. Properties of the most popular origami patterns for engineering applications [37].

PATTERN	RIGID	1 DOF	FLAT	MULTISTABILITY	GEOMETRY
Miura-ori	Yes	Yes	Yes	Yes	Surface
Waterbomb	Yes	Yes	No	Yes	Cone
Yoshimura	Yes	Yes	Yes	No	Cylinder
Kresling	No	No	Yes	Yes	Cylinder
Flasher	Yes	Yes	No	No	Surface

DoF: degree of freedom.

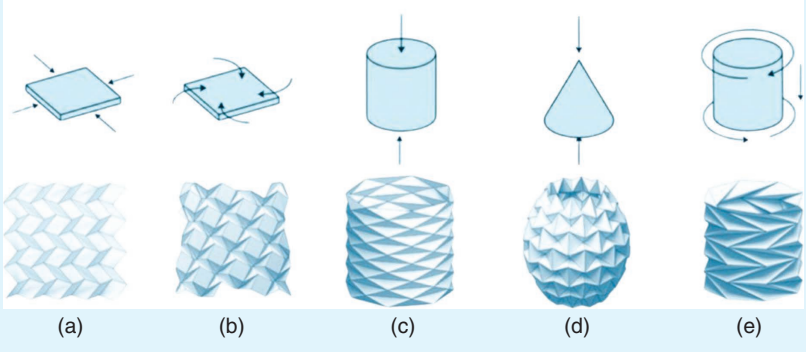

FIGURE 1. Representation of origami-based structures: (a) Miura-ori for compact folding, (b) Flasher for radial expansion, (c) Yoshimura for cylindrical stability, (d) Waterbomb for versatile compression, and (e) Kresling for torsional deformation. Adapted from [38].

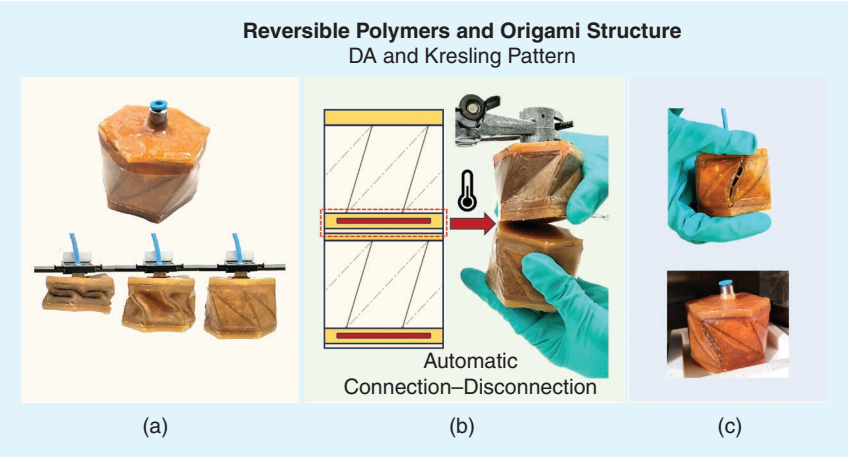

FIGURE 2. Proposal for a modular and reconfigurable soft robot. (a) Soft modular actuator. (b) Modularity with an automatic connector interface. (c) Healing properties possible with the use of reversible polymers.

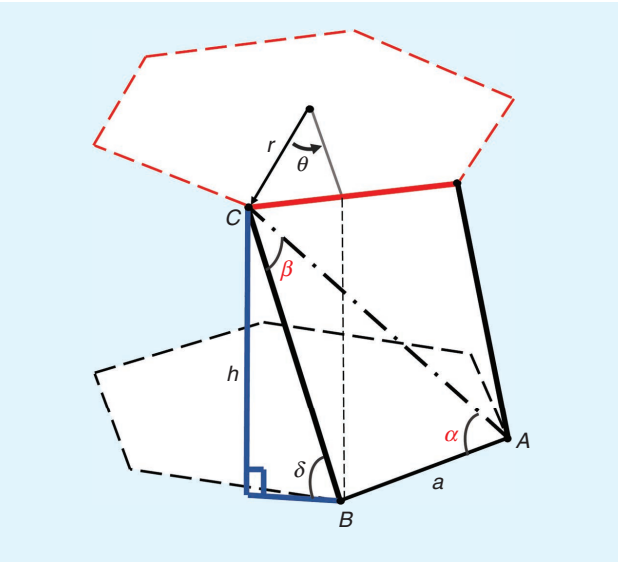

FIGURE 3. Origami Kresling pattern showcasing its intricate geometrical components.

solar panel design for space applications [39]. These patterns do not produce a link-like structure and are therefore not considered further in this article. The Waterbomb, Yoshimura, and Kresling patterns have a folding geometry that generates cylindrical-like structures. The Waterbomb and Yoshimura patterns are discarded because they only have one degree of freedom (1 DoF), and the Yoshimura pattern lacks multistable behavior. Therefore, the Kresling pattern, which offers the most advantageous features, is ideal for creating modular, reconfigurable, and soft robotic structures, as explored in this article.

The article is organized as follows. The soft module actuator design, materials, and fabrication will be described in the next section. The section "Soft Connector for Robot Modularity" addresses the soft connector approach for robot modularity. The section "Experimental Setup and Methodology" provides details on the experimental setups and methodologies. These will be used in the section "Tests and Results," which will address the actuator characterization and evaluate the performance of the proposed MSR in two different configurations: 1) the robot with two identical modules made of self-healing material (SHM) and 2) the robot with one module made of SHM and another module made of polypropylene (PP). Finally, the main conclusions of the work, together with some future works, are described in the section "Conclusions." Figure 2 summarizes the general contents of this study.

SOFT ACTUATOR MODULE

The essential criteria for the design and manufacturing of soft robots are determined by the choice of physical structures and materials, both for the robot body and for its operation. In this case, an origami-based structure was chosen as the physical structure for each module actuator, and a thermoreversible polymer based on DA networks was chosen as the manufacturing material.

This section describes the design and materials for the manufacturing of the soft actuator and the characterization of its operation.

SOFT ACTUATOR DESIGN

The primary movements in nature are bending, twisting, and contraction/extension. In robotics, mimicking natural motion is a main objective, so foldable structures based on origami include intrinsic contraction/extension displacements in the most popular patterns for robotics, such as Muira-ori, Yoshimura, Flasher, or Kresling [37]. However, Kresling presents an additional DoF, including twisting. This property enhances the origami structure by introducing a bistable behavior, exclusive of this pattern. In this work, the Kresling pattern is proposed to create a soft actuator as the main module of the MSR. It is a sequence of triangles determined by the base line a and the angles α and β (see Figure 3). The 2D pattern is described by (1), which defines the relationships among L_{AB}, L_{BC}, and L_{AC}. By contrast, the 3D Kresling structure is governed by (2), detailing the motion and variation in edge lengths l_{AB}, l_{BC}, and l_{AC}.

According to a previous work [40], a configuration with $\alpha = 38°$, $\beta = 30°$, $n = 6$, and $a = 30$ mm is optimal for the performance of the bistable behavior of the Kresling pattern. The bistable behavior is one of the most interesting properties of this pattern, implying that the structure has two functional states: folded and unfolded. This behavior generates a rotation on the central axis of the structure, through the angle θ [see (4)]. The height h of the origami structure

changes as it rotates, based on the angle of folding δ, as described by (5).

$$\begin{aligned} L_{AB} &= a \\ L_{BC} &= \frac{a \cdot \sin(\alpha)}{\sin(\beta)} \\ L_{AC} &= \frac{a \cdot \sin(\alpha+\beta)}{\sin\beta} \end{aligned} \tag{1}$$

$$\begin{aligned} l_{AB} &= 2r\sin\left(\frac{\pi}{n}\right) \\ l_{BC} &= \sqrt{h^2 - 2r^2\cos\theta + 2r^2} \\ l_{AC} &= \sqrt{h^2 - 2r^2\cos\left(\frac{2\pi}{n+\theta}\right) + 2r^2} \end{aligned} \tag{2}$$

$$r = \frac{\frac{a}{2}}{\sin\left(\frac{\pi}{n}\right)} \tag{3}$$

$$\theta = \frac{2\pi}{n} - 2\sin^{-1}\left(\frac{l_{BC}\cos\delta}{2r}\right) \tag{4}$$

$$h = l_{BC} \cdot \sin(\delta). \tag{5}$$

SOFT ACTUATOR DEVELOPMENT

MATERIALS

DA polymers consist of a reversible polymer network in which the crosslinks are formed by the equilibrium DA reaction, which introduces both a self-healing capacity and reprocessability in the polymer. In case of damage, the reversible DA bonds are mechanically broken, and reactive furan and maleimides groups are formed, bringing the material locally out of equilibrium. These reactive groups have the tendency to rebind back to reform the DA bond when the fracture surfaces are brought back in contact. Consequently, when the equilibrium is reformed, the mechanical performance and functionality of these materials is completely restored. In addition, the self-healing capacity is also completely recovered, and therefore multiple damage–healing cycles can be carried out at exactly the same damaged location, with only a slight loss of strength. Traditional elastomers are bonded together by permanent covalent bonds, making it impossible to unbond, reshape, or reform them. As a result, these traditional polymers are not suitable for recycling. By contrast, dynamic covalent networks, like the DA polymers used in this work with thermoreversible bonds, offer recyclability [41], [42].

The DA networks to be used in this work are formed using two monomers: bismaleimide (DPBM) and a furan-functionalized Jeffamine. The crosslink bonds are dynamic due to the fact that the DA reaction between a furan and a maleimide is an equilibrium reaction. To enhance the molecular mobility within the network, there are two options available: 1) the crosslink density can be decreased or the molecular weight of the furan-functionalized compound can be raised; 2) the maleimide-to-furan (r) ratio can be decreased, and a deficit of reactive maleimide components can be used in the synthesis [43]. Adjusting this ratio will impact the crosslink density, which in turn will affect the mechanical properties of the network. The r-ratio also plays a key role in determining the gel transition temperature. Networks with a reduced r-ratio will transition to a more fluid state at lower temperatures, facilitating reshaping and reprocessing at lower temperatures [44]. More details on the synthesis process can be found in the supplementary materials of [45] and [46]. An important advantage of DA is that it enables the creation of materials of different stiffnesses with the possibility of varying self-healing properties.

FABRICATION

The origami-based actuator structure has been built with DA elastomeric polymers. The actuator cylinder, structured like origami, requires flexibility to adapt to the pattern configuration during its performance. For this reason, a DPBM-FT5000-r0.5 DA network was used, while DA DPBM-FT3000-r1 was selected for the top and bottom covers, which hold the structure together, keeping the hexagonal design and making it not susceptible to deformation. The synthesis of the material was made using the values presented in Table 2, where a value of 13 g was used for the cylinder and 10 g for each cover. According to [43], the mechanical properties for these DA polymers show an elasticity modulus of 0.12 MPa and 139 MPa, respectively. The significant difference is due to the use of longer furan compounds with higher molecular weight and a reduction in the r-ratio, resulting in a substantial decrease in crosslink density and, consequently, a significant decrease in Young's modulus [43].

The material obtained from the synthesis is liquid (165 °C) before it is cured [47]. It is poured onto silicone molds (Dragon skin 20), and it takes approximately 24 h to fully cure. The process for obtaining the functional actuator is shown in Figure 4. It has the following five general steps:

1) *Pattern*: To obtain the pattern with DA [see Figure 4(a)], a silicone mold was first created and then paper triangles

TABLE 2. Reagents used for the DA synthesis and their mechanical properties.

DA NETWORK	TGEL (°C)	MTOTAL (G)	MALEIMIDE (G)	FURAN (G)	INHIBITOR (G)	E (MPA)
DPBM-FT5000-r0.5	90	13	1.01	11.98	0.05	0.12
DPBM-FT3000-r1	128	10	2.14	7.85	0.107	139

mTotal: total mass.

corresponding to the pattern were placed on the mold. The DPBM-FT5000-r0.5 was carefully poured on top of this. Later, once the DA was cured, it was demolded and placed on another mold to pour DA on the other side of the paper, embedding the paper. The DPBM-FT5000-r0.5 is a soft material that enables the folding behavior of the origami, while the paper parts allow the structure to retain the geometry of the pattern.

2) *Pattern joint*: One of the main features of the origami is its ability to transform a 2D pattern into a 3D structure. In this case, the structure is obtained by simply joining the edge at the beginning of the pattern with the edge at the end, as shown in Figure 4(b). This connection was made using the self-healing properties of the DA. Four clamps were required to maintain the alignment of the edges.
3) *Cylinder*: Once the outer sides of the pattern have been joined together, a polyhedral cylinder is obtained, as presented in Figure 4(c). Now the cylinder shape is almost circular; therefore, to keep its original geometry, two hexagonal pieces are needed as covers for the top and bottom of the cylinder.
4) *Top and bottom covers*: The two hexagonal covers were constructed using the same steps to create the pattern. DPBM-FT3000-r1, a more rigid material, was used to embed the paper. A 4-mm-diameter pneumatic connector was attached to the top cover to operate the structure by vacuum pressure [see Figure 4(d)].
5) *Actuator*: Finally, the polyhedral cylinder and the covers were joined to obtain an airtight origami actuator [see Figure 4(e)]. The self-healing properties of the DA were once again applied to bond the actuator parts together using a thin layer of DPBM-FT5000-r0.5.

SOFT CONNECTOR FOR ROBOT MODULARITY

As described previously, soft modular robot designs allow them to be easily reconfigured and repaired without complications. This study proposes a modular robot with flexible modules and joints, including an automatic connection/disconnection process between modules. The section "Soft Actuator Model" discussed the design and validation of the soft module, whereas this section details the proposed connector for the MSR.

The DA self-healing polymer includes the property of reprocessability, which means that the material can be reused via thermal processing [48]. This feature was exploited to create an interface that acts as a connector that is able to join different soft modules of the MSR.

CONNECTOR DESIGN

The diagram shown in Figure 5(a) describes our modularity approach. The origami actuator represents each module, and the connection interface consists of a heating mat embedded in one of the outer faces of the actuator [see Figure 5(b)].

The heating mat is the essential element for providing thermal excitation to the thermoreversible material, allowing it to reach the appropriate temperature levels for the degelled state. This mat is embedded together with a thermocouple sensor into the connection interface, which is built with DPBM-FT3000-r1 using the same hexagonal geometry of the origami top and bottom covers. The heater has a diameter of 50 mm; it is powered by 12 V, and its power is 2 W.

As illustrated in Figure 5(a), this consists of the origami module, the junction interface at one of its terminals embedded in DPBM-FT3000-r1, and finally a layer of DPBM-

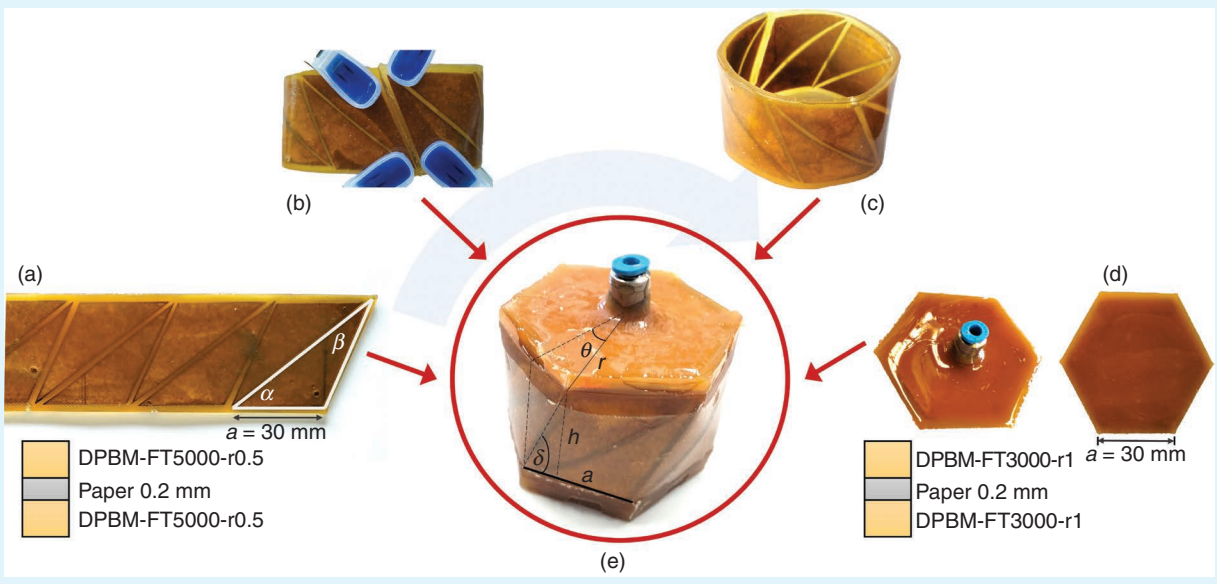

FIGURE 4. Manufacturing process of the soft actuator based on origami structure. (a) Kresling pattern creation with paper triangles embedded using soft DA SHM. (b) Joining the edges of the pattern to achieve the 3D structure of the actuator. (c) Polyhedral cylinder. (d) Cover manufacturing with paper hexagons embedded using hard DA SHM. (e) Origami actuator prototype.

FT3000-r0.5, which is actually the junction material due to its property of being a reversible polymer.

EXPERIMENTAL SETUP AND METHODOLOGY

The natural state of the origami actuator is unfolded, and vacuum pressure is used to fold and unfold the module. The actuator is characterized by applying various vacuum pressure values. A test bench has been set up to measure the linear displacement in response to changes in pressure.

The vacuum air source is provided by coupling a vacuum generator to an air compressor. An SMC vacuum regulator, with an operating range from 0 to –100 kPa, is connected between the generator and the pneumatic connection of the actuator to vary the air pressure. The displacement was determined by the visual tracking of the actuator movement, using a millimeter scale on the back of the actuator as a reference.

After establishing the operating range of the actuator, this is tested to determine the load to which it can be subjected. A Tinius Olsen model 5ST tensile test machine was used to register the actuator behavior. Pneumatic suction custom-made clamps were used to attach the actuator to the machine, one of them with a mechanism that allows the origami free rotation. Figure 6 shows the design of the top and bottom clamps. The top clamp includes the free rotation mechanism; thus, three parts are required. 1) There is a mechanical connection with the tensile machine, through a locking bar. This part also has a hole to allow the vacuum connection for a suction cup. 2) There is a rotation component, whose design is based on a cylinder with an inner hexagon that makes a cavity, which will act as a suction cup to hold the origami module. In the center, it contains a hole through which the vacuum air tube will lead, acting as an axis of rotation. 3) There is a support component of the mobile piece. This part and the first one are joined by four screws, creating a cage for the mobile part. On the other hand, the bottom clamp also includes a mechanical connection to fix it to the

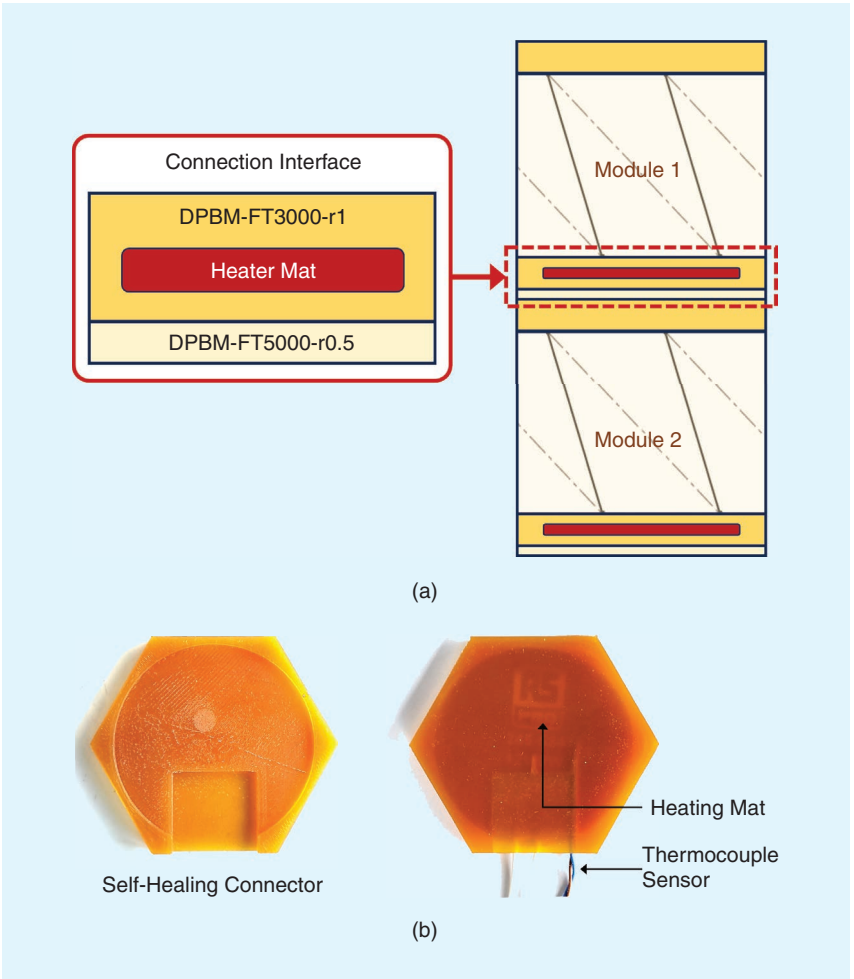

FIGURE 5. Connection interface for modularity. (a) Diagram. The origami actuator represents each module. A heating mat is embedded in one of the module covers and acts as a connection interface. (b) Real. The heating mat and thermocouple sensor embedded using DA material.

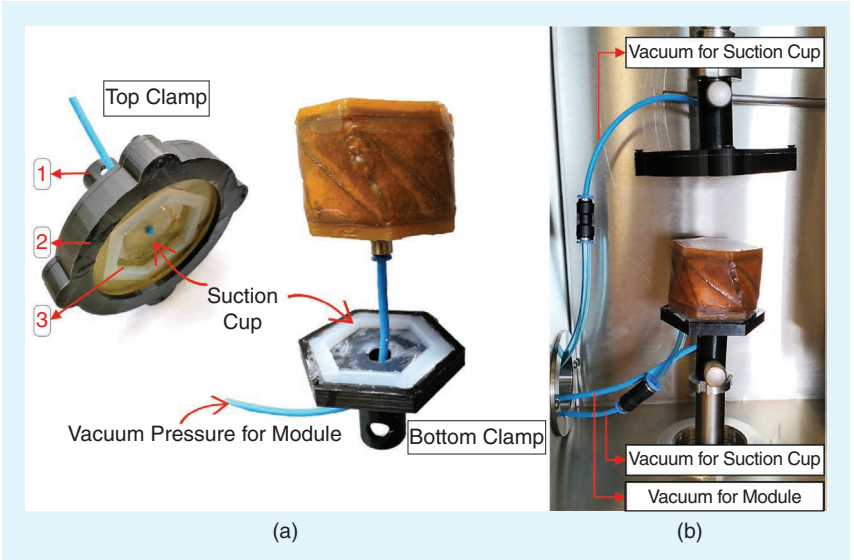

FIGURE 6. (a) Tensile test setup. (b) Installation of suction cup clamps to hold the module in the tensile tests, and vacuum supply ducts.

tensile machine as well as two vacuum supply ducts, one for the suction cup and another to actuate the module. The suction cup is obtained by a hexagon cavity similar to the free mobile piece.

TESTS AND RESULTS

ACTUATOR CHARACTERIZATION

Once the origami-based soft module is created, it is characterized as an actuator. The test was performed as follows. The origami actuator starts in a fully deployed position, with a total height of 58 mm, including the top and bottom covers. Once the vacuum pressure is applied, the origami folds according to its Kresling pattern, as shown in Figure 7(a). The linear displacement is evident, and for the rotational behavior, a red arrow shows the movement of one of the edges. Figure 7(a) also illustrates that the fold is produced with a displacement of 30.5 mm when the pressure is between 0 kPa and –15 kPa. As the pressure decreases to less than –15 kPa, the actuator still folds, but only to a small extent, with a displacement difference of 4.7 mm between –15 kPa and –80 kPa. Therefore, the proper folding and unfolding behavior of the origami actuator occurs in the range from 0 kPa to –15 kPa.

To determine the load capacity of the actuator, it must be actuated at a known pressure. Based on previous tests, a pressure of –10 kPa will be used. At this pressure, with no external force applied, the actuator is fully folded, which is its initial position for this test. The internal pressure of the actuator will remain constant throughout the test. Note that by choosing –10 kPa instead of the limit of –15 kPa, a safer and more reliable operating condition is ensured, extending the actuator's life span and maintaining a consistent performance.

The test was programmed at a speed of 0.83 mm/s and ran up to 200% of elongation (actuator totally deployed). Figure 7(b) shows the machine in the corresponding elongation states of the tensile test and the test results. The blue axis represents the force (in Newtons) and the red axis the elongation (%), both in terms of displacement (in millimeters).

The results show that the force is maintained at an average of 17.16 N, and finally it reaches a maximum value of 23.28 N. When the elongation reaches a value of 160%, the origami becomes fully deployed, reaching its maximum geometrical displacement. From here on, the tension applied deforms the actuator geometry, and the internal pressure of the chamber inflates the actuator. This is the reason why the force increases from here until the test finishes at 200% of elongation.

The results of the characterization show that the actuator can function with vacuum air at a pressure of about –10 kPa and can withstand up to 17 N, equivalent to carrying loads of up to 1.73 kg without causing deformation of the geometry of the module.

CONNECTION PERFORMANCE

The MSR is created by joining at least two origami modules, one of which must contain the connection interface. Figure 8(a) illustrates the process of connecting the modules for the first time, with the addition of the DPBM-FT3000-r0.5 layer.

A 2-g thin layer of DPBM-FT5000-r0.5 material is poured onto one side of a module [A in Figure 8(a)], and the material is spread evenly over its surface [B in Figure 8(a)]. This material is softer than DPBM-FT3000-r1 and has better self-healing

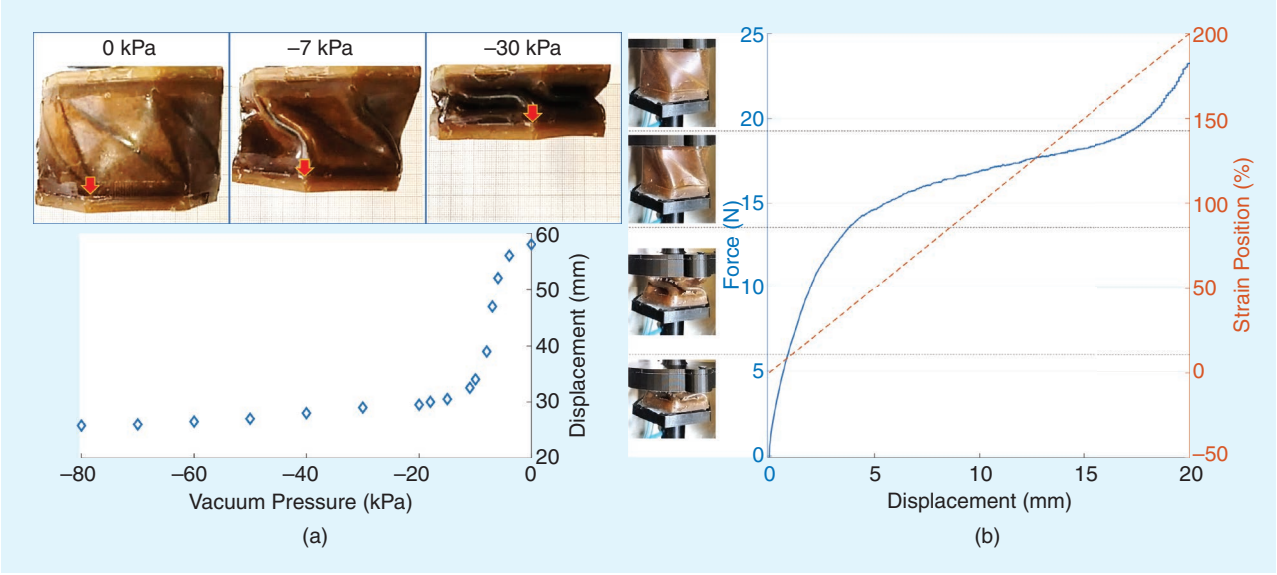

FIGURE 7. Actuator characterization. (a) Pressure tests. Physical test from initial resting position to folded position and characterization curve: displacement according to the vacuum pressure applied. The origami reaches the folding position with a displacement of 30.5 mm, which corresponds to an internal pressure of between –10 kPa and –15 kPa. The remaining pressure values to –80 kPa represent minimum displacement. (b) Tensile tests with –10-kPa inner pressure and physical states of the actuator during the tensile test at –10 kPa. The actuator is attached to the tensile machine by custom-made clamps. The force and elongation results are represented with blue and red lines, respectively.

properties, which allows the modules to be connected and disconnected in such a way that their structures do not suffer collateral damage from the coupling. Next, the face of the second origami containing the heating mat is placed on the treated side of the first module [C of Figure 8(a)]. The connection is fulfilled when the DA material is cured, after about 24 h under ambient conditions.

To separate the modules, the heater will warm up the connection interface until it reaches an optimal temperature to get the thermoreversible gelation in the DA material, which allows a reversible transition from a liquid state to a gel state when heated [49]. This temperature is in the range of 80–120 °C. A temperature control was implemented using an Arduino Mega board and an IRF540NPbF MOSFET to activate the heater by a pulsewidth modulation signal, and a type-K thermocouple with an I2C amplifier module as a sensor to close the control loop. The controller used is a proportional-integral-derivative controller with gains $Kp = 350$, $Ki = 0.01$, and $Kd = 2$. This proper control of the temperature will allow the material to bond and debond as many times as necessary for modules connection and disconnection.

The disconnection performance is shown in Figure 8(b), where a manual disconnection is carried out. The MSR is attached at its upper part by a clamp to the demonstrator. The top module includes the connection interface. A thermal camera is used to record the temperature variations during the whole process. The temperature target for the control loop is 100 °C, and the joint heats up slowly because of the heater's low power (2 W). The surface of the connector registers about 50 °C according to the thermal camera, while the internal thermocouple sensor reaches about 90 °C. With these parameters, the separation of the modules starts. The performance can be done manually; it only requires fixing one of the modules and applying a light pulling force.

To quantify the force required to disconnect the modules, a tensile test was performed using the same machine and clamps used for the actuator characterization tests. Once the target temperature is reached, the tensile test begins. The test results are presented in Figure 9, showing that the force to separate the modules is 25 N with a machine displacement of 4 mm during 4.27 min.

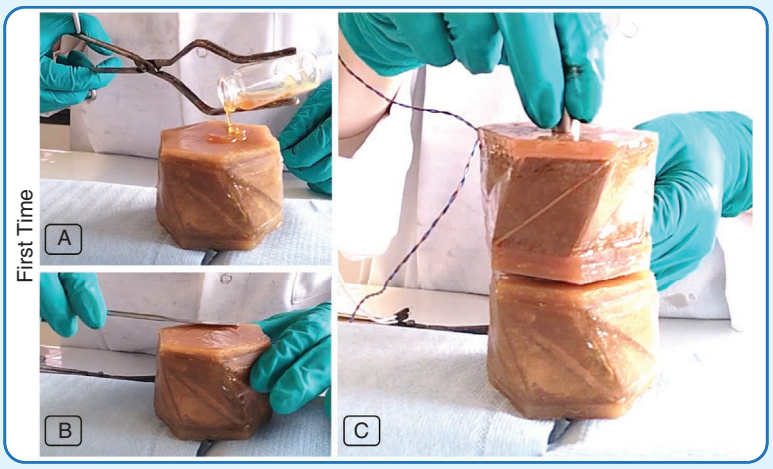

FIGURE 8. Module connection–disconnection process. (a) Connection: DPBM-FT5000-r0.5 is poured and spread between the modules to allow thermoreversible gelation in the DA. (b) Disconnection: Manual disconnection and thermal images during the disconnection process.

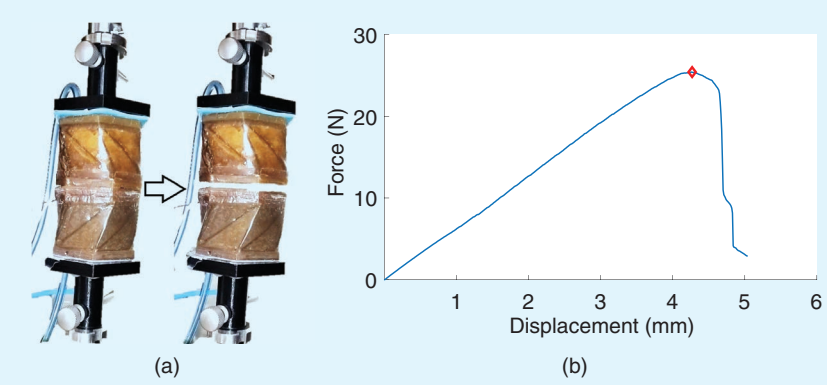

FIGURE 9. Performing a tensile test to disconnect the modules. (a) MSR attached to the tensile machine. (b) Experimental results. The force (blue line) required to separate the modules is 25 N, with a displacement of about 4 mm during a time of 4.27 min.

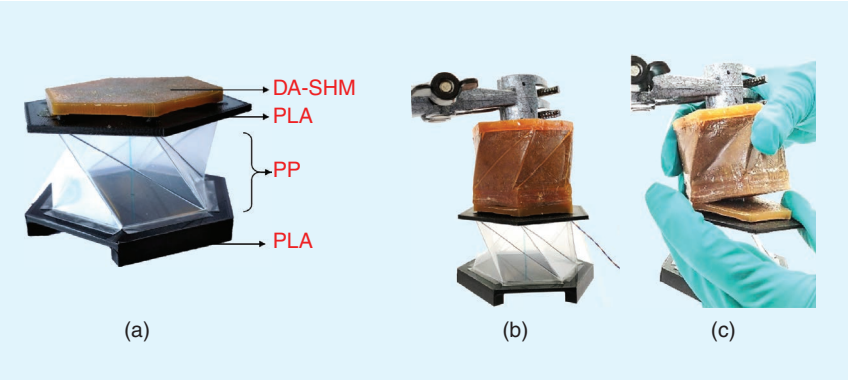

FIGURE 10. MSR made of two different modules. (a) PP module with a DPBM-FT3000-r1 layer. (b) SHM module connected to PP module. (c) Disconnection of the two modules.

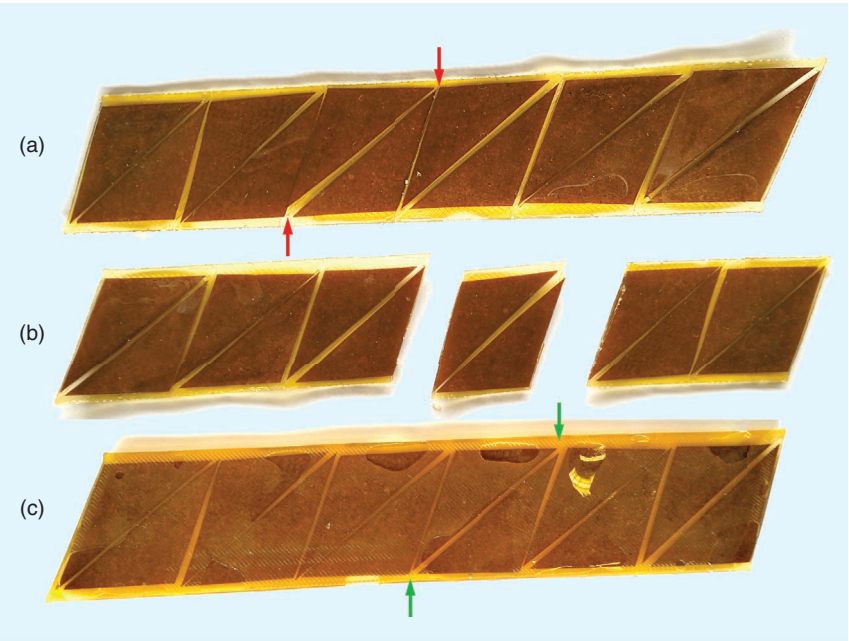

FIGURE 11. Reconfiguration process of the SHM module by realigning its pattern by cutting and healing.

To rebond the modules, we follow the same procedure as for separating them: 1) activate the heater of the bonding interface until it reaches a temperature of about 80 °C; 2) once the DPBM-FT3000-r0.5 layer is sticky, bond the second module directly, ensuring that both are aligned.

To enhance the scalability, functionality, and versatility of the flexible connection interface for MSRs, we propose to implement the interface in other flexible modules. Specifically, the flexible module designed in [50] is used, which follows the same origami Kresling pattern used in this work but is made of a different material and has another actuation system. The module comprises a PP sheet attached to 3D-printed covers made of polylactic acid (PLA) to maintain the geometry and is actuated by a tendon.

This module has been selected to demonstrate that the interface can be used beyond modules of the same material, as proposed with DA.

In this instance, a DPBM-FT3000-r1 layer was added to the top of the PP module, as shown in Figure 10. This is the only requirement to establish a link between the connection interface and another module. For this test, a PP module and a DA module are used. The connection and disconnection of the modules were carried out following the same procedures explained previously for the two DA modules—equally successfully.

To show the modularity approach in a visual way, a video of the connection interface development and testing is available at https://vimeo.com/880558310.

RECONFIGURATION AND HEALING PROPERTIES VALIDATION

The healing capability of the MSR was used to repair and reconfigure the origami actuator, demonstrating the versatility and sustainability of the SHMs. Two cases were tested: one to reconfigure the origami module realigning its pattern and the second to repair different damages on the actuator.

The first reconfiguration case is shown in Figure 11, and it has three stages.

1) In the process to build the actuator where the Kresling pattern was created by embedding paper in DA material, once the DA material was cured, we figured out an important misalignment of the triangles [marked in red in Figure 11(a)], which implied an error in the pattern and therefore in the module behavior.
2) A blade was used to cut the misaligned triangles and separate them from the pattern [Figure 11(b)].
3) The paper was embedded in just one face. To complete the embedding process, the pattern was mounted into the respective silicone mold by aligning all of the triangles. Then, the SHM was poured. Finally, once the material was cured, the origami pattern achieved a fine alignment [marked in green in Figure 11(c)]. The resulting pattern shown in Figure 11(c) is rotated 180° with respect to the pattern in Figure 11(a); it is the reverse side of the latter.

Additionally, the self-healing property of the material has been used to repair damages on the actuator structure. The actuator is powered by vacuum pressure and must be airtight; otherwise, it will not work properly. Two additional tensile tests were carried out, one with a –20-kPa inner pressure and the other with –30 kPa. In the –20-kPa test, the actuator suffered from some shearing and cracking, particularly at the

edges of the origami, where most of the pressure is generated in the geometry.

For large fissures, where a complete edge was damaged, it was necessary to apply additional DA material with a local temperature of about 120 °C. To ensure a proper healing, the entire structure was later heated in an oven at a temperature of 60 °C for about 2 h [see Figure 12(a)]. The repair of the module with a significant cut in the origami pattern was performed using such a procedure because of two important considerations. First, the origami pattern contains embedded pieces of paper and is not a complete panel of SHM, and second, to achieve correct curing without adding additional material, the cut must be aligned and a slight pressure must be applied, which is not feasible on the assembled actuator as it is a 3D structure with acute edges. For small fissures, it was only required to apply a low temperature in the fissures, without the use of extra material.

The repaired actuator was used for the third tensile test at a –30-kPa inner pressure. Based on the initial test results [see Figure 7(b)], it was found that the average operating range of the actuator was about 100% strain; therefore, the third test was programmed with 100% strain at a speed of 0.83 mm/s. Figure 12(b) displays the two tests conducted at different inner pressures (–20 kPa and –30 kPa) represented by yellow and purple lines, respectively. The module has been successfully repaired, achieving an average force value of 12.28 N.

CONCLUSIONS

An innovative MSR has been proposed in this work in which the thermal reversibility of the DA-based self-healing polymer constituting its structure allows its flexibility, scalability, and reconfigurability in a simple and robust way.

A key feature of the robot is that its modules can connect and disconnect through a novel connector installed in one of their covers, which allows the DA network to be thermally stimulated. The connection interface is built with a reusable SHM based on a thermoreversible DA reaction that embeds a heating layer to allow the connection–disconnection through temperature variation. The temperature control system implemented in the robot makes the module disassembly possible in an automatic and robust way. The connector performance was tested and validated in an MSR in two configurations: modularity with two SHM modules and modularity with one SHM module and another PP module. The force to separate the modules was 25 N, and 24 h were required to connect them again—the time needed for the material to fully cure.

The design of the modules is another key feature of the robot. They are soft actuators based on an origami structure that implements the Kresling pattern to allow the actuation (linear displacement plus rotation) through vacuum pressure.

The origami is made of a DA-based self-healing polymer in a process that embeds paper into the structure to provide the needed structural consistency while maintaining its flexibility. Both the design and the SHM ensure the reconfigurability and healing of the module when it suffers from fissures that can affect its performance.

The characterization of the actuator module was addressed in an experiment that relates the linear displacement of the origami with the vacuum pressure inside its body. The reconfiguration and healing capabilities were also demonstrated through several experimental tests in which the origami pattern was restored after a pattern misalignment and a severe edge fissure was totally cured.

Future work includes the reconfiguration of the origami pattern using the features of SHMs. The Kresling geometry can be generated in two orientations: one as presented in this study, with the angle of rotation θ in a clockwise direction; the other with the angle of rotation θ in a counterclockwise direction, for which the 2D pattern would be a mirror image

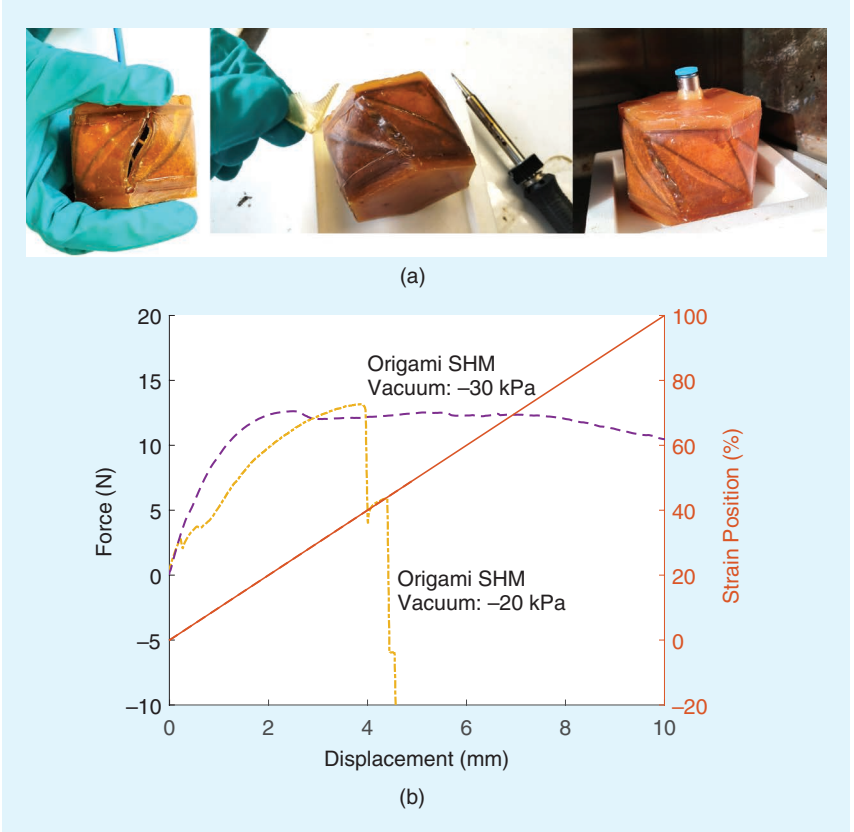

FIGURE 12. SHM repair and test. (a) Repair process of large fissures in the self-healing actuator: adding additional material and healing in an oven at 60 °C for 2 h. (b) Tensile test results of force and elongation. Test at –20 kPa, where actuator edges cracked (yellow line). Test at –30 kPa with the actuator healed (purple line).

of the previous one. The actuator would be able to change its rotation angle just by cutting the pattern joint and healing in the reverse direction of the pattern. This configuration would allow the whole rotation of the origami to be canceled when two modules are joined, providing only a linear displacement, which can be required in a wide range of applications. Other applications, such as artificial muscles or crawling robots, can benefit from the enhanced rotational capabilities achieved by varying the pattern configuration of each module and the number of them connected in the chain. Undoubtedly, each particular application will require the integration of sensors to monitor the robot state and the design of a specific control system to improve the robot performance. All of this is to be addressed in future work to further demonstrate the impact of the approaches presented here in real robotic applications.

In conclusion, this proposal presents several technological opportunities for soft robots, such as the following:

1) *Modular design*: This design allows for customizable and repairable designs for soft robots, adding robustness.
2) *Reconfiguration*: This strategy is used to adapt soft robots to changing functional requirements. It includes the possibility of reusing robotic systems, providing efficiency and versatility.
3) *Self-healing*: This is a transformative solution to the fragility of soft robots. Self-healing mechanisms can mitigate vulnerabilities and significantly extend the lifetime of soft robots, making them economically competitive and environmentally sustainable.
4) *New manufacturing methods that use folding and binding*: These techniques are advantageous for space exploration and remote access applications, making production processes more efficient through compact sheet transportation and in situ fabrication. These technologies contribute to accessibility and scalability in soft robotics.

ACKNOWLEDGMENT

This research has been supported by the project SOFIA, with reference PID2020-113194GB-I00, funded by MCIN/AEI/10.13039/501100011033, and the project ADAPTA, with reference PLEC2023-010218, funded by MCIN/AEI/10.13039/501100011033. Lisbeth Mena is the corresponding author.

AUTHORS

Lisbeth Mena, Department of Systems Engineering and Automation, Carlos III University of Madrid, 28911 Madrid, Spain. E-mail: lmena@pa.uc3m.es.

Seppe Terryn, Brubotics, Vrije Universiteit Brussel and imec, 1050 Brussels, Belgium. E-mail: seppe.terryn@vub.be.

Bram Vanderborght, Brubotics, Vrije Universiteit Brussel and imec, 1050 Brussels, Belgium. E-mail: bram.vanderborght@vub.be.

Concepción A. Monje, Department of Systems Engineering and Automation, Carlos III University of Madrid, 28911 Madrid, Spain. E-mail: cmonje@ing.uc3m.es.

REFERENCES

[1] C. Zhang, P. Zhu, Y. Lin, Z. Jiao, and J. Zou, "Modular soft robotics: Modular units, connection mechanisms, and applications," *Adv. Intell. Syst.*, vol. 2, no. 6, 2020, Art. no. 1900166, doi: 10.1002/aisy.201900166.

[2] E. R. Perez-Guagnelli, S. Nejus, J. Yu, S. Miyashita, Y. Liu, and D. D. Damian, "Axially and radially expandable modular helical soft actuator for robotic implantables," in *Proc. IEEE Int. Conf. Robot. Automat. (ICRA)*, Piscataway, NJ, USA: IEEE Press, 2018, pp. 4297–4304, doi: 10.1109/ICRA.2018.8461239.

[3] H. Gu et al., "Self-folding soft-robotic chains with reconfigurable shapes and functionalities," *Nature Commun.*, vol. 14, no. 1, 2023, Art. no. 1263, doi: 10.1038/s41467-023-36819-z.

[4] B. T. Phillips et al., "A dexterous, glove-based teleoperable low-power soft robotic arm for delicate deep-sea biological exploration," *Sci. Rep.*, vol. 8, no. 1, 2018, Art. no. 14779, doi: 10.1038/s41598-018-33138-y.

[5] B. S. Homberg, R. K. Katzschmann, M. R. Dogar, and D. Rus, "Haptic identification of objects using a modular soft robotic gripper," in *Proc. IEEE/RSJ Int. Conf. Intell. Robots Syst. (IROS)*, Piscataway, NJ, USA: IEEE Press, 2015, pp. 1698–1705, doi: 10.1109/IROS.2015.7353596.

[6] A. K. Mishra, E. Del Dottore, A. Sadeghi, A. Mondini, and B. Mazzolai, "SIMBA: Tendon-driven modular continuum arm with soft reconfigurable gripper," *Front. Rob. AI*, vol. 4, Feb. 2017, Art. no. 4, doi: 10.3389/frobt.2017.00004.

[7] D. Drotman, S. Jadhav, M. Karimi, P. de Zonia, and M. T. Tolley, "3D printed soft actuators for a legged robot capable of navigating unstructured terrain," in *Proc. IEEE Int. Conf. Robot. Autom. (ICRA)*, Piscataway, NJ, USA: IEEE Press, 2017, pp. 5532–5538, doi: 10.1109/ICRA.2017.7989652.

[8] A. Rafsanjani, Y. Zhang, B. Liu, S. M. Rubinstein, and K. Bertoldi, "Kirigami skins make a simple soft actuator crawl," *Sci. Rob.*, vol. 3, no. 15, 2018, Art. no. eaar7555, doi: 10.1126/scirobotics.aar7555.

[9] R. K. Katzschmann, J. DelPreto, R. MacCurdy, and D. Rus, "Exploration of underwater life with an acoustically controlled soft robotic fish," *Sci. Rob.*, vol. 3, no. 16, 2018, Art. no. eaar3449, doi: 10.1126/scirobotics.aar3449.

[10] S. Kurumaya et al., "A modular soft robotic wrist for underwater manipulation," *Soft Rob.*, vol. 5, no. 4, pp. 399–409, 2018, doi: 10.1089/soro.2017.0097.

[11] A. D. Horchler et al., "Peristaltic locomotion of a modular mesh-based worm robot: Precision, compliance, and friction," *Soft Rob.*, vol. 2, no. 4, pp. 135–145, 2015, doi: 10.1089/soro.2015.0010.

[12] M. A. Robertson and J. Paik, "New soft robots really suck: Vacuum-powered systems empower diverse capabilities," *Sci. Rob.*, vol. 2, no. 9, 2017, Art. no. eaan6357, doi: 10.1126/scirobotics.aan6357.

[13] L. Mena, J. Muñoz, C. A. Monje, and C. Balaguer, "Modular and self-scalable origami robot: A first approach," *Mathematics*, vol. 9, no. 12, 2021, Art. no. 1324, doi: 10.3390/math9121324.

[14] J.-Y. Lee and K.-J. Cho, "Development of magnet connection of modular units for soft robotics," in *Proc. 14th Int. Conf. Ubiquitous Robots Ambient Intell. (URAI)*, Piscataway, NJ, USA: IEEE Press, 2017, pp. 65–67, doi: 10.1109/URAI.2017.7992886.

[15] J. Zou, Y. Lin, C. Ji, and H. Yang, "A reconfigurable omnidirectional soft robot based on caterpillar locomotion," *Soft Rob.*, vol. 5, no. 2, pp. 164–174, 2018, doi: 10.1089/soro.2017.0008.

[16] L. S. Novelino, Q. Ze, S. Wu, G. H. Paulino, and R. Zhao, "Untethered control of functional origami microrobots with distributed actuation," *Proc. Natl. Acad. Sci.*, vol. 117, no. 39, pp. 24,096–24,101, 2020, doi: 10.1073/pnas.2013292117.

[17] M. E. Sayed, J. O. Roberts, R. M. McKenzie, S. Aracri, A. Buchoux, and A. A. Stokes, "Limpet II: A modular, untethered soft robot," *Soft Rob.*, vol. 8, no. 3, pp. 319–339, 2021, doi: 10.1089/soro.2019.0161.

[18] Z. Jiao, C. Zhang, W. Wang, M. Pan, H. Yang, and J. Zou, "Advanced artificial muscle for flexible material-based reconfigurable soft robots," *Adv. Sci.*, vol. 6, no. 21, 2019, Art. no. 1901371, doi: 10.1002/advs.201901371.

[19] L. Wang and F. Iida, "Towards "soft" self-reconfigurable robots," in *Proc. 4th IEEE RAS & EMBS Int. Conf. Biomed. Robot. Biomechatronics (BioRob)*, Piscataway, NJ, USA: IEEE Press, 2012, pp. 593–598, doi: 10.1109/BioRob.2012.6290258.

[20] J. Germann, M. Dommer, R. Pericet-Camara, and D. Floreano, "Active connection mechanism for soft modular robots," *Adv. Rob.*, vol. 26, no. 7, pp. 785–798, 2012, doi: 10.1163/156855312X626325.

[21] A. López-Díaz, J. De La Morena, F. Ramos, E. Vázquez, and A. S. Vázquez, "A novel hydrogel-based connection mechanism for soft modular robots," in *Proc. Int. Conf. Robot. Automat. (ICRA)*, 2022, pp. 7124–7130, doi: 10.1109/ICRA46639.2022.9812164.

[22] H. Wang, S. Terryn, Z. Wang, G. Van Assche, F. Iida, and B. Vanderborght, "Self-regulated self-healing robotic gripper for resilient and adaptive grasping," *Adv. Intell. Syst.*, vol. 5, no. 12, 2023, Art. no. 19013712300223.

[23] J. Legrand, S. Terryn, E. Roels, and B. Vanderborght, "Reconfigurable, multi-material, voxel-based soft robots," *IEEE Trans. Robot. Autom.*, vol. 8, no. 3, pp. 1255–1262, Mar. 2023, doi: 10.1109/LRA.2023.3236883.

[24] J. Legrand, E. Roels, and B. Vanderborght, "Easy integrability and data processing of a soft tactile array sensor through reconfiguration," *IEEE Sensors J.*, vol. 23, no. 7, pp. 7719–7727, Apr. 2023, doi: 10.1109/JSEN.2023.3250947.

[25] A. Firouzeh and J. Paik, "An under-actuated origami gripper with adjustable stiffness joints for multiple grasp modes," *Smart Mater. Struct.*, vol. 26, no. 5, 2017, Art. no. 055035, doi: 10.1088/1361-665X/aa67fd.

[26] J. Santoso, E. H. Skorina, M. Luo, R. Yan, and C. D. Onal, "Design and analysis of an origami continuum manipulation module with torsional strength," in *Proc. IEEE/RSJ Int. Conf. Intell. Robots Syst. (IROS)*, Piscataway, NJ, USA: IEEE Press, 2017, pp. 2098–2104, doi: 10.1109/IROS.2017.8206027.

[27] K. Kuribayashi et al., "Self-deployable origami stent grafts as a biomedical application of Ni-rich TiNi shape memory alloy foil," *Mater. Sci. Eng.: A*, vol. 419, nos. 1–2, pp. 131–137, 2006, doi: 10.1016/j.msea.2005.12.016.

[28] S. A. Zirbel, M. E. Wilson, S. P. Magleby, and L. L. Howell, "An origami-inspired self-deployable array," in *Proc. Conf. Smart Mater., Adaptive Struct. Intell. Syst.,* vol. 56031, pp. 1–6, 2013, doi: 10.1115/SMASIS2013-3296.

[29] M. Koryo, "Method of packaging and deployment of large membranes in space," *Inst. Space Astronautical Sci. Rep.*, vol. 618, pp. 1–9, Dec. 1985.

[30] J. P. Gardner et al., "The James Webb space telescope," *Space Sci. Rev.*, vol. 123, no. 4, pp. 485–606, 2006, doi: 10.1007/s11214-006-8315-7.

[31] N. K. Mandsberg, J. F. Christfort, K. Kamguyan, A. Boisen, and S. K. Srivastava, "Orally ingestible medical devices for gut engineering," *Adv. Drug Delivery Rev.*, vols. 165–166, pp. 142–154, May 2020, doi: 10.1016/j.addr.2020.05.004.

[32] A. J. Taylor, Y. Chen, M. Fok, A. Berman, K. Nilsson, and Z. T. H. Tse, "Cardiovascular catheter with an expandable origami structure," *J. Med. Devices*, vol. 11, no. 3, 2017, Art. no. 034505, doi: 10.1115/1.4036581.

[33] Z. Song et al., "Origami lithium-ion batteries," *Nature Commun.*, vol. 5, no. 1, 2014, Art. no. 3140, doi: 10.1038/ncomms4140.

[34] P. M. Njogu et al., "Evaluation of planar inkjet-printed antennas on a low-cost origami flapping robot," *IEEE Access*, vol. 8, pp. 164,103–164,113, 2020, doi: 10.1109/ACCESS.2020.3020824.

[35] Z. Zhakypov and J. Paik, "Design methodology for constructing multimaterial origami robots and machines," *IEEE Trans. Robot.*, vol. 34, no. 1, pp. 151–165, Feb. 2018, doi: 10.1109/TRO.2017.2775655.

[36] C. H. Belke and J. Paik, "Mori: A modular origami robot," *IEEE/ASME Trans. Mechatronics*, vol. 22, no. 5, pp. 2153–2164, Oct. 2017, doi: 10.1109/TMECH.2017.2697310.

[37] M. Meloni et al., "Engineering origami: A comprehensive review of recent applications, design methods, and tools," *Adv. Sci.*, vol. 8, no. 13, 2021, Art. no. 2000636, doi: 10.1002/advs.202000636.

[38] L. M. Fonseca, G. V. Rodrigues, and M. A. Savi, "An overview of the mechanical description of origami-inspired systems and structures," *Int. J. Mech. Sci.*, vol. 223, Jun. 2022, Art. no. 107316, doi: 10.1016/j.ijmecsci.2022.107316.

[39] S. Yogesh, M. Yogalakshmi, M. Abishek, R. A. Prasath, and G. Madhusudanan, "Origami based folding techniques for solar panel applications," *Int. J. Elect. Eng. Technol.*, vol. 12, no. 3, pp. 158–164, 2021.

[40] L. Mena, C. A. Monje, and C. Balaguer, "Origami kresling pattern as soft scalable link," in *Jornadas Robótica, Educación Automática Bioingeniería*, 2022, pp. 70–74.

[41] B. Briou, B. Améduri, and B. Boutevin, "Trends in the Diels–Alder reaction in polymer chemistry," *Chem. Soc. Rev.*, vol. 50, no. 19, pp. 11,055–11,097, 2021, doi: 10.1039/D0CS01382J.

[42] S. Terryn et al., "A review on self-healing polymers for soft robotics," *Mater. Today*, vol. 47, pp. 187–205, Jul./Aug. 2021, doi: 10.1016/j.mattod.2021.01.009.

[43] S. Terryn, J. Brancart, E. Roels, G. Van Assche, and B. Vanderborght, "Room temperature self-healing in soft pneumatic robotics: Autonomous self-healing in a Diels-Alder polymer network," *IEEE Robot. Autom. Mag.*, vol. 27, no. 4, pp. 44–55, Dec. 2020, doi: 10.1109/MRA.2020.3024275.

[44] S. Terryn, E. Roels, J. Brancart, G. Van Assche, and B. Vanderborght, "Self-healing and high interfacial strength in multi-material soft pneumatic robots via reversible Diels–Alder bonds," *Actuators*, vol. 9, no. 2, 2020, Art. no. 34, doi: 10.3390/act9020034.

[45] S. Terryn, J. Brancart, D. Lefeber, G. Van Assche, and B. Vanderborght, "Self-healing soft pneumatic robots," *Sci. Rob.*, vol. 2, no. 9, 2017, Art. no. eaan4268, doi: 10.1126/scirobotics.aan4268.

[46] E. Roels, S. Terryn, P. Ferrentino, J. Brancart, G. Van Assche, and B. Vanderborght, "An interdisciplinary tutorial: A self-healing soft finger with embedded sensor," *Sensors*, vol. 23, no. 2, 2023, Art. no. 811, doi: 10.3390/s23020811.

[47] E. Roels, S. Terryn, J. Brancart, G. Van Assche, and B. Vanderborght, "A multi-material self-healing soft gripper," in *Proc. 2nd IEEE Int. Conf. Soft Robot. (RoboSoft)*, Piscataway, NJ, USA: IEEE Press, 2019, pp. 316–321, doi: 10.1109/ROBOSOFT.2019.8722781.

[48] E. Roels et al., "Processing of self-healing polymers for soft robotics," *Adv. Mater.*, vol. 34, no. 1, 2022, Art. no. 2104798, doi: 10.1002/adma.202104798.

[49] F. Tanaka, "Theory of thermoreversible gelation," *Macromolecules*, vol. 22, no. 4, pp. 1988–1994, 1989, doi: 10.1021/ma00194a077.

[50] L. Mena, J. Muñoz, C. A. Monje, S. Martínez de la Casa, and C. Balaguer, "Study of an origami structure as a soft link," in *XLIV Jornadas de Automática. Universidade da Coruña*. Zaragoza, Spain: Servizo de Publicacións, Sept. 2023, pp. 650–654.